Glassy behavior induced by geometrical frustration in a hard-core lattice gas model

M. Weigt[1](*) and Alexander K. Hartmann[1](**)

[1] *Institute for Theoretical Physics, University of Göttingen - Bunsenstr. 9, D-37073 Göttingen, Germany*

PACS. 64.70.Pf – Glass transitions.
PACS. 05.70.Jk – Critical point phenomena.

Abstract. – We introduce a three-dimensional hard-core lattice-gas model and investigate numerically its compaction behavior. If compactified slowly, the system undergoes a discontinuous crystallization transition. If compactified much faster, the system stays in a meta-stable liquid state and undergoes a glass transition under further compaction. We show analytically and numerically that a naive Bethe-Peierls approach fails to describe the observed behavior. Generalizing the latter by taking into account local loops, the transitions found in the three-dimensional model are well represented.

The last decades have seen a great interest in understanding the structural glass transition [1, 2]. Experimentally, the latter is defined by a dramatic dynamical slowing down which prevents the systems from reaching a crystalline equilibrium state at experimental time scales. A central role in theoretical approaches was played by fully connected spin-glass models with multi-spin interactions [2–5]. These models in fact show a purely dynamical transition towards a glassy state followed by a thermodynamic transition at lower temperature. The dynamical transition, even if not strictly present in real materials due to activated processes, is believed to present some similarities to the structural glass transition.

The analogies between fully connected spin glasses and structural glasses are, however, of purely phenomenological nature, missing a microscopic verification. The main differences for spin-glass models are, that they have multi-spin interaction, which in addition are disordered (quenched disorder) and long-ranged (fully connected models). So, in particular, these models do not have any crystalline state.

Recently, some of these points could be cured by considering models based on Bethe lattices or Husimi trees, which are the analogon of Bethe lattices for multi-spin interactions: On finite length scales, these lattices have no inhomogeneities. The corresponding models undergo a crystallization transition which was found to be of first order in most of the interesting cases. By cooling or compactifying these models relatively fast, the system stay in the meta-stable liquid (or paramagnetic) phase. In analogy to their fully-connected counterparts, they undergo

(*) E-mail: weigt@theorie.physik.uni-goettingen.de
(**) E-mail: hartmann@theorie.physik.uni-goettingen.de

a dynamical glass transition at even lower temperature, which is followed by a thermodynamic transition [6–8]. The latter cannot be observed in simulations (or experiments) since the system does not equilibrate below the dynamical transition. These models still have, however, the problem of having multi-spin interactions (which, in some cases, are introduced by local constraints concerning more than two particles, as seen in [8]).

In this letter, we first present a three-dimensional lattice-gas model with pure two-particle interactions which is numerically found to show a dynamical slowing down reminiscent to the glass transition in liquids of hard particles or Lennard Jones liquids [9]. This glass transition is introduced by geometrical frustration [10] which prohibits constructing a globally dense configuration from purely local rules. Furthermore, we present a generalized Bethe approximation: Whereas a straight forward Bethe approximation neglects geometrical frustration and leads to a completely different physical picture, we have to take into account short loops existing in the model. Doing this, we find a behavior which is very close to the one seen numerically on the three-dimensional lattice.

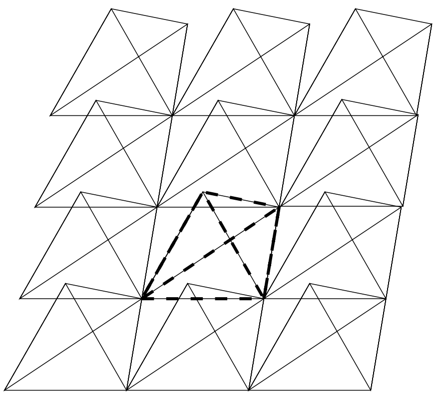

Fig. 1

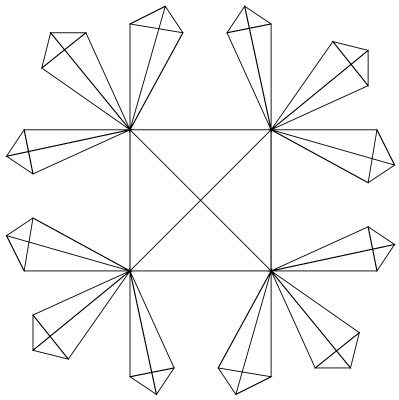

Fig. 2

Fig. 1 – One layer of the considered three-dimensional lattice. The unit-cell, as marked by the dashed lines, is a regular tetrahedron which is translated along its edges.

Fig. 2 – Part of the generalized Bethe lattice used to analytically approximated the three-dimensional lattice. The unit cell, which is equivalent to a complete graph of four vertices, and the co-ordination number are kept, whereas further loops of finite length are neglected.

We consider a three-dimensional lattice of $N = L^3$ sites. It can be generated from a tetrahedron which is translated along its edges, see Fig. 1. We impose periodic boundary conditions in the direction of three edges of a tetrahedron which start from one corner. Sites can be occupied by at most one particle, $x_i \in \{0, 1\}$. These are assumed to have a hard core of radius one, i.e. no two neighboring sites can be occupied simultaneously. Every tetrahedron can thus carry at most one particle, the other sites are forbidden by the hard-core constraint. The maximal density is thus bound from above by 0.25.

Geometrical frustration enters via short loops. This becomes obvious if we try to construct the densest crystalline state by locally dense packings. If we start with a single particle, its neighboring sites have to be empty. We would like to put new particles on second neighbors to achieve a locally close packing. Some of these second neighbors are, however, connected by links, and thus cannot be simultaneously selected as particle positions. The resulting arbitrarity in selecting occupied second neighbors finally leads to globally disordered packings of sub-maximal density.

The thermodynamic properties of the model are given by the grand-canonical partition function

$$\Xi = \sum_{\{x_i\}\in\mathcal{C}} e^{\mu\sum_i x_i} \tag{1}$$

which sums over the set $\mathcal{C}$ of allowed configurations fulfilling the hard-core constraint. The chemical potential μ is coupled to the total particle number and can be used to tune the particle density to any value. In our system, we study the compaction of the model which can be achieved by increasing μ. In particular, densest packings are reached in the limit $\mu \to \infty$.

To start with, we numerically study the behavior of the model using Monte Carlo (MC) simulations up to size $N = 50^3$. For each MC step, a site i is selected randomly. With probability $p = 0.5$ a MOVE (M) step is performed, and with probability $1-p$ an EXCHANGE (EX) step:

M If site i is empty and has exactly one occupied neighbor, the particle is moved to i. In all other cases, the configuration remains unchanged.

EX If the site is occupied, the particle is removed with probability $\exp(-\mu)$. If the site is empty, and all neighboring sites are empty, a particle is placed on i.

Note that in this way detailed balance is fulfilled, and the equilibrium distribution is the one corresponding to eq. (1). All simulations start with $\mu = 0$. Then μ is increased in steps of $\delta\mu = 0.1$. For every value of the chemical potential, we perform $n_{\rm MC}N$ Monte-Carlo steps.

For small μ the system is in a liquid phase: All particles are free to move around, they are not localized, and the time average over the density does not depend on the site.

For very slow compaction, we observe a discontinuous crystallization transition at $\mu \simeq 2$, cf. Fig. 3. At this point, the symmetry between sites breaks down, every tetrahedron has one site with higher than average density, and three of lower density. The average density exhibits a discontinuity and quickly approaches 0.25, i.e. its theoretically maximal value, if we further increase μ. The first order character of this transition can be numerically tested by decreasing μ again. Doing this we observe a hysteresis, cf. Fig. 3, the system stays in the crystalline state even for $\mu < 2$.

If, starting from the liquid state at low μ, we increase μ quite fast, crystallization is avoided. The system stays in the meta-stable liquid state, even if the crystalline one is globally stable. This phenomenon appears in analogy to a super-cooled liquid. At higher μ, the system starts to freeze into a glassy state, being characterized by a density which is much smaller than 0.25. This asymptotic density depends heavily on the compaction rate.

Is it possible to understand this behavior in terms of a Bethe-Peierls approximation? This approximation consists in replacing the three-dimensional lattice by a locally tree-like lattice of fixed co-ordination 12, i.e. of the co-ordination of the original lattice. This model, however, does not show the same behavior: All transitions, i.e. the crystallization as well as the glass transition, are continuous, cf. [11] for the corresponding model with fluctuating connectivities, and the MC compaction dynamics on a Bethe lattice easily finds the closest hard-sphere packing [12]. The problem is that this approximation neglects all short loops, and thus the local geometrical frustration. Also the closest crystalline packing has the wrong density $\rho = 1/2$.

This problem can be circumvented if we go back to the construction of the three-dimensional lattice from a tetrahedron. In graph-theoretical language, a tetrahedron is a complete graph

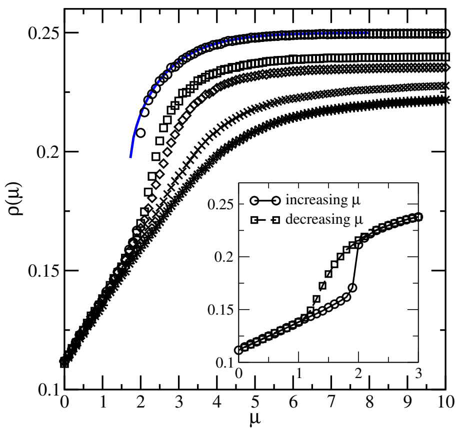

Fig. 3

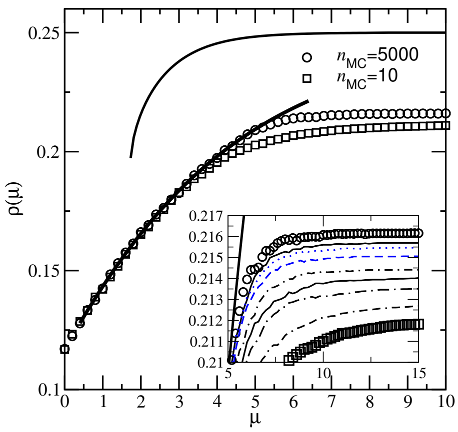

Fig. 4

Fig. 3 – Density ρ as a function of the chemical potential μ for $n_{\rm MC} = 1, 2, 5, 25, 1000$ Monte-Carlo sweeps per value of the chemical potential (from bottom to top). All $n_{\rm MC}$ sweeps, the chemical potential is increased by 0.1. The data are for one run of a lattice with $N = 50^3$ sites. The solid line represents the analytical approximation for the crystalline phase presented below. Inset: Density ρ as a function of μ for slowly increasing ($n_{\rm MC} = 500$) and subsequently fast decreasing ($n_{\rm MC} = 5$) chemical potential.

Fig. 4 – Density ρ as a function of the chemical potential μ for the numerical simulation of random graphs consisting of tetrahedrons ($p = 4$, $K = 3$) of size $N = 999$, averaged over 100 graphs. Here $\delta\mu = 0.2$ was used. The solid lines show analytical results. The inset shows the behavior for high values of μ for $n_{\rm MC}$ ranging from 5000 (top curve) to 10 (bottom), again together with the analytical result (left).

of four vertices, or a 4-clique. In every lattice site, four of the cliques meet. If we preserve this structure, but neglect finite loops formed by edges from different tetrahedrons, see Fig 2, we arrive at a generalized Bethe lattice which still leads to a solvable mean-field model. Due to the fully connected character of the 4-cliques, the model preserves, however, the geometrical frustration: 2nd neighbors of any selected site are paired in connected groups of 3 vertices belonging to the same clique.

The model can be solved most easily using the cavity method [13] which, in the liquid as well as in the crystalline state, reduced to the Bethe-Peierls iterative method. Please note, however, that the latter is modified with respect to the presence of short loops. On a coarse-grained level, where every local clique is considered as one object, the graph becomes locally tree-like and therefore solvable by an iterative procedure. In the following, we use this coarse-grained tree-like structure and speak about trees, branches etc. only in this sense. We also introduce a slightly generalized setting: The graph is constructed by joining $K + 1$ cliques of size p in every vertex. Our original model is given by $K = 3$ and $p = 4$. The cliques are numbered by $\nu = 1, ..., (K + 1)N/p$. We closely follow the presentation and notation of [13], cf. also [8].

Let us consider a branch of the graph which is rooted in vertex i. One of the cliques containing vertex i is not part of the branch, we denote it by ν. We first calculate the partition function $\Xi_{0/1}(i, \nu)$ of this branch where i is fixed to be empty ($x_i = 0$) or occupied ($x_i = 1$). Let us denote the other K cliques containing i by $\nu_1, ..., \nu_K$, and the further vertices contained in clique ν_k by $j_{1,k}, ..., j_{p-1,k}$, $k = 1, ..., K$. Due to the hard-sphere constraint, every clique is allowed to carry at most one particle, we thus find

$$\begin{aligned}\Xi_0(i,\nu) &= \prod_{k=1}^{K}\left[\prod_{a=1}^{p-1}\Xi_0(j_{a,k},\nu_k)+\sum_{a=1}^{p-1}\Xi_1(j_{a,k},\nu_k)\prod_{b\neq a}\Xi_0(j_{b,k},\nu_k)\right]\\ \Xi_1(i,\nu) &= e^{\mu}\prod_{k=1}^{K}\left[\prod_{a=1}^{p-1}\Xi_0(j_{a,k},\nu_k)\right]\ . \end{aligned}\tag{2}$$

Introducing the cavity fields $\mu h_i^\nu = \ln(\Xi_1(i,\nu)/\Xi_0(i,\nu))$, these iterate according to

$$\begin{aligned} h_i^\nu &= 1+\sum_{k=1}^{K} u(h_{j_{1,k}}^{\nu_k},...,h_{j_{p-1,k}}^{\nu_k})\\ u(h_1,...,h_{p-1}) &= -\frac{1}{\mu}\ln\left(1+\sum_{a=1}^{p-1}e^{\mu h_a}\right)\ , \end{aligned}\tag{3}$$

i.e. they result thus as linear superpositions of the local chemical potential μ and fields propagated along the cliques. The true effective field on a vertex is given by the contributions propagated from all neighbors, i.e. from all $K+1$ cliques containing the vertex, $H_i = 1+\sum_{k=1}^{K+1} u(h_{j_{1,k}}^{\nu_k},...,h_{j_{p-1,k}}^{\nu_k})$. Note that the right-hand site of this equation still contains the fields h_j^ν coming from single branches only. The distribution of these fields serves as an order parameter and allows to identify liquid, crystalline and glassy states. Furthermore, its knowledge allows to calculate the grand canonical potential [13], with $\mathcal{E}$ denoting the set of all p-cliques in the graph,

$$A = -\ln\Xi = -K\sum_i \ln\left(1+e^{\mu H_i}\right)+\sum_{\nu\in\mathcal{E}}\ln\left(1+\sum_{i\in\nu}e^{\mu h_i^\nu}\right)\tag{4}$$

as well as the average particle density per site

$$\rho = \frac{\overline{\sum_i x_i}}{N} = \frac{1}{N}\sum_i \frac{e^{\mu H_i}}{1+e^{\mu H_i}}\ .\tag{5}$$

The liquid phase, which is expected to be globally stable for small chemical potential μ, is characterized by its translational invariance. The effective fields h_i^ν and consequently H_i do not depend on the site index i and are thus given by the fixed point of Eq. 3.

This translational invariance breaks down spontaneously in the crystalline phase: On each clique, there is one site of higher average density, all the other $(p-1)$ vertices have a homogeneous lower density. There are thus two different fields $h^{(1)} < h^{(2)}$, which are a solution of

$$\begin{aligned} h^{(1)} &= 1+K\ u(h^{(2)},h^{(1)},...,h^{(1)})\\ h^{(2)} &= 1+K\ u(h^{(1)},...,h^{(1)})\ . \end{aligned}\tag{6}$$

We observe that, for $p\geq 3$ and $K\geq 2$, this solution appears discontinuously at a spinodal point μ_s. Still, its grand canonical potential is larger than the one of the liquid phase. The two potentials cross at the crystallization transition $\mu_\mathrm{c} > \mu$s, which thus describes a first-order transition which is accompanied by a discontinuous change in the density. Sending $\mu\to\infty$, the crystalline system quickly approaches the maximal density 1/4. The spinodal and transition points for our model with $p = 4$ and $K = 3$ are given by $\mu_{\mathrm{s}} \simeq 1.73$ and $\mu_{\mathrm{c}} \simeq 2.18$.

The liquid phase stays, however, meta-stable even above μ_{c} describing thus a super-cooled liquid. If we compactify the system rather quickly, it stays liquid, and thus in local equilibrium. At higher density, the system even falls out of this meta-stable equilibrium: An exponential number of glassy states of smaller density (and higher grand canonical potential) appears discontinuously at a dynamical transition μ_{d} and traps the system. At μ_{rsb} a sub-exponential number of glassy states finally reaches lower grand canonical potential than the liquid one. For $p = 4$ and $K = 3$ we find $\mu_{\mathrm{d}} \simeq 5.7$ and $\mu_{\mathrm{rsb}} \simeq 6.1$.

Technically, this can be either seen by applying the functional replica approach in the one-step replica symmetry broken ansatz [14], or by equivalently using the cavity approach which generalizes the Bethe-Peierls solution to more than one state [13]. In [7] a quite general derivation was given which is directly applicable to the hard-core lattice gas. The main difference to the liquid solution is that, in different pure states, there are different effective fields h_i^ν. They can be characterized by their histograms $P_i^\nu(h)$. Assuming that the equivalence of sites is not broken in the ensemble of pure states, all $P_i^\nu(h)$ are identical and fulfill the equation

$$\begin{aligned} \frac{P(h)}{(1+e^{\mu(h-1/(K+1))})^m} &= \lambda_m \int \prod_{a=1}^{p-1} \prod_{k=1}^{K} \frac{dh_{a,k}\; P(h_{a,k})}{(1+e^{\mu(h_{a,k}-1/(K+1))})^m} \prod_{k=1}^{K} \left[1 + \sum_{a=1}^{p-1} e^{\mu h_{a,k}} \right]^m \\ &\quad \times \delta\left(h - 1 - \sum_{k=1}^{K} u(h_{1,k}, ..., h_{p-1,k}) \right) \end{aligned} \tag{7}$$

with λ_m being a normalization constant, and m the usual one-step replica symmetry breaking parameter [15]. This equation can be easily solved numerically using the population-dynamical algorithm proposed in [13]. Once we know $P(h)$, the distribution of true fields H_i, the grand canonically potential and the density can be calculated easily. The dynamical transition point μ_{d} can be identified by the discontinuous appearance of a non-trivial solution to Eq. 7 at $m = 1$, whereas the static transition μ_{rsb} is given by the point where the replica-symmetry broken grand canonical potential becomes globally stable with respect to the liquid one [16].

In Fig. 4, these findings are compared with numerical simulations obtained on fixed-connectivity random graphs built from 4-cliques. Note that in principle the value of μ_{d} can be inferred from extrapolating to infinitesimal slow compaction ($n_{\mathrm{MC}} \to \infty$). However, our data turned out to be incompatible with every form of fits we have tried. Nevertheless, the analytical curve crosses the $\rho(\infty)$ line for $n_{\mathrm{MC}} = 5000$ at a value of $\mu \simeq 5.7$, which coincides with the analytical prediction for μ_{d}. Note also that we numerically do not observe the crystallization transition. This results from the disordered global structure of the random graph which contains long random loops of length $\mathcal{O}(\ln N)$ which are not consistent with the crystalline structure. These loops are not existent in the translationally invariant three-dimensional model. Comparing the analytical data of the Bethe-Peierls approach with the numerical ones obtained in three dimensions, we find a good coincidence of the liquid solution for small μ and the crystalline for larger μ. Deviations are due to the approximate nature of the analytical approach. One major difference between the three-dimensional and the mean-field model is the gap between glassy states and the crystalline one. Being rather large in the mean-field case, it is not clear if a finite gaps exists in finite dimensions.

To conclude, we have introduced a three-dimensional hard-core lattice-gas model which shows a discontinuous crystallization transition as well as glassy behavior if super-cooled sufficiently fast. To reproduce this behavior analytically in a mean-field treatment, it was necessary to go beyond the naive Bethe approximation which neglects all short loops in the system. These loops, and the resulting geometrical frustration, are responsible for the physical behavior of the model. Taking it into account, a generalized mean-field model is introduced which shows the characteristic features of the glass transition known from fully connected multi-spin-interaction models. If super-cooled, the system falls out of equilibrium at a dynamical transition which is accompanied by the appearance of an exponential number of states. Also in our model, this transition is not of thermodynamic nature, a replica-symmetry breaking equilibrium transition occurs only at higher chemical potential.

This approach shows, that the understanding of the behavior of the three-dimensional model can be achieved only if relevant local structures, short loops in our case, are taken into account. It would thus be interesting to go beyond the analysis presented here, and to take systematically into account more and more complex structures. Even if being still of mean-field nature, we expect the results to be more and more precise in the description of the model in finite dimensions. This could e.g. clarify the open question of the existence of a finite density gap between glassy and crystalline states.

Another interesting conclusion concerns the typical numerical hardness of the vertex-cover problem, which is equivalent to finding dense hard-sphere packings [11]: Graphs containing small loops, or geometrical frustration, are expected to be much harder to cover with a small vertex cover size than locally tree-like graphs like random graphs. This opens the interesting question in how far local structures may influence the global hardness of a combinatorial problem.

* * *

We acknowledge interesting an fruitful discussions with J. Berg, F. Ricci-Tersenghi, and R. Zecchina. AKH obtained financial support from the DFG (Deutsche Forschungsgemeinschaft) under grants Ha 3169/1-1 and Zi 209/6-1. MW thanks the ICTP Trieste for hospitality.

REFERENCES

[1] For review see, W. Götze, *Liquids, freezing and glass transition*, Les Houches (1989), J.P. Hansen, D. Levesque, J. Zinn-Justin eds, North Holland; C.A. Angell, Science **267**, 1924 (1995).
[2] J-P. Bouchaud, L.F. Cugliandolo, J. Kurchan and M. Mezard, in *Spin Glasses and Random Fields*, ed. by A.P. Young (World Scientific, Singapore, 1998).
[3] T.R. Kirckpatrick and D. Thirumalai, Phys. Rev. B **36**, 5388 (1987).
[4] A. Crisanti, H. Horner and H.J. Sommers, Z. Physik **92**, 173 (1993).
[5] L.F. Cugliandolo and J. Kurchan, Phys. Rev. Lett. **71**, 173 (1993).
[6] S. Franz, M. Mézard, F. Ricci-Tersenghi, M. Weigt, and R. Zecchina, Europhys. Lett. **55**, 465 (2001).
[7] S. Franz, M. Leone, F. Ricci-Tersenghi, and R. Zecchina, Phys. Rev. Lett. **87**, 127209 (2001).
[8] G. Biroli and M. Mézard, Phys. Rev. Lett. **88**, 025501 (2002).
[9] W. Kob, J. Phys. Cond. Matter **11**, R85 (1999).
[10] D.R. Nelson and F. Spaepen, Solid State Physics **42**, 1 (1989).
[11] M. Weigt and A.K. Hartmann, Phys. Rev. E **63**, 056127 (2001).
[12] J. Berg and F. Ricci-Tersenghi, private communication.
[13] M. Mézard and G. Parisi, Eur. Phys. J. B **20**, 217 (2001).
[14] R. Monasson, J. Phys. A **31**, 513 (1998).
[15] M. Mézard, G. Parisi and M.A. Virasoro, *Spin Glass Theory and Beyond* (World Scientific, Singapore, 1987).
[16] R. Monasson, Phys. Rev. Lett. **75**, 2847 (1995).